

MDPI

Article

The Quasistatic Pressure Characteristics of a Confined Cabin in a Water Mist Environment

Ya Zhang ^{1,2}, Xiaobin Li ^{1,2}, Xiuyi Xi ^{1,2}, Mengzhen Li ^{1,2}, Yiheng Zhang ^{1,2}, Hai Huang ^{1,2} and Wei Chen ^{1,2,*}

- Hubei Defense Science and Technology Key Laboratory of Ship Explosion Damage and Protection, Wuhan University of Technology, Wuhan 430063, China
- School of Naval Architecture, Ocean and Energy Power Engineering, Wuhan University of Technology, Wuhan 430063, China
- * Correspondence: whutcw01@126.com

Abstract: To investigate the quasistatic pressure load characteristics of an explosion in a confined cabin in a water mist environment, explosion tests were conducted under different explosive and water mist masses. The concentration of water mist, droplet diameter, and quasistatic pressure inside the cabin were measured. On the basis of the theoretical model of quasistatic pressure in adiabatic ideal gas cabins, a theoretical model of the quasistatic pressure in a confined cabin in a water mist environment was established. On the basis of experimental data and theoretical models, an empirical formula was proposed for the peak quasistatic pressure of implosion in a water mist environment. A model for a cabin explosion in a water mist environment was established, and the load characteristics of a cabin explosion under high water mist concentrations were analyzed. The relevant research results contribute to the prediction of the quasistatic pressure of explosions in a confined cabin in a water mist environment.

Keywords: confined cabins; implosion test; water mist concentration; quasistatic pressure; empirical equations



Citation: Zhang, Y.; Li, X.; Xi, X.; Li, M.; Zhang, Y.; Huang, H.; Chen, W. The Quasistatic Pressure Characteristics of a Confined Cabin in a Water Mist Environment. *J. Mar. Sci. Eng.* **2024**, *12*, 1650. https://doi.org/10.3390/jmse12091650

Academic Editor: Joško Parunov

Received: 6 August 2024 Revised: 5 September 2024 Accepted: 13 September 2024 Published: 14 September 2024



Copyright: © 2024 by the authors. Licensee MDPI, Basel, Switzerland. This article is an open access article distributed under the terms and conditions of the Creative Commons Attribution (CC BY) license (https://creativecommons.org/licenses/by/4.0/).

1. Introduction

When an explosion occurs inside a ship cabin, the impact load characteristics are dramatically different from those in open spaces [1–3]. Chronologically, the explosion pressure inside a cabin can be divided into two parts. One part is shock wave pressure with a high peak pressure but a short duration of action. The other part is quasistatic pressure, which has a low peak pressure but a long duration. Research indicates that the damage caused by quasistatic pressure to cabin structures cannot be ignored [4–6].

Several studies have been conducted on quasistatic pressure load characteristics. Trott et al. [7] reported that quasistatic pressure is the main reason for damage to closed containers during tests. Weibull [8] and Esparala et al. [9] proposed a parameter closely related to the peak quasistatic pressure, which is the ratio of charge to container (m/V). Anderson et al. [10] derived a formula for calculating quasistatic pressure through dimensional analysis. Zhang et al. [11] adopted specialized quasistatic test components to measure the quasistatic pressure after a TNT explosion in a confined cabin. Based on the previously published experimental data, an empirical formula was fitted for the peak quasistatic pressure in a confined cabin. Many protective methods have been proposed to reduce the damage of internal explosion loads to structures. Water mist has received increasing attention as a new type of green environmental protection method. Willauer et al. [12] conducted internal explosion tests on large-sized compartments under different water mist concentrations, and the results indicate that the greater the concentration of water mist in the confined space, the greater the weakening of water mist in the explosion load. Chen et al. [13] carried out experiments in an explosion chamber of 990 mm \times 224 mm \times 464 mm. The results show that the peak overpressure of the initial shock wave, the peak overpressure

of the reflected shock wave and the quasi-static pressure all decrease because of the existence of water mist, the attenuation rates are 31.55%, 72.87% and 77.78% respectively. Kong et al. [14] measured the quasistatic pressures of three different doses of TNT during an explosion in a closed cabin under high-concentration water mist ($70 \pm 10 \, \text{g/m}^3$). These results suggest that the reduction and increase in the static pressure peak caused by water mist increase with an increasing TNT dosage. Existing theories [15–17] have indicated that the weakening of explosive loads by water mist mainly stems from two aspects. First, when the initial shock wave passes over the water mist, momentum transfer occurs between the shock wave and the droplet, resulting in responses such as motion, deformation, and fragmentation of the droplet. The initial shock wave and subsequent reflected waves are ultimately weakened. Second, owing to the evaporation effect of droplets absorbing a large amount of energy from the combustion of detonation products, the ambient temperature decreases. In addition, a large amount of water vapor decreases the oxygen content in the confined space and inhibits post-combustion reactions, thus reducing quasistatic pressure.

However, systematic experimental verification of the weakening of the explosion pressure in confined spaces by fine water mist is lacking. In addition, an empirical formula for rapidly predicting the quasistatic pressure of explosions in confined spaces in water mist environments has not yet been proposed. Therefore, this work will conduct explosion tests in a confined cabin with and without a water mist environment, establish a theoretical model for the quasistatic pressure of a cabin explosion in a water mist environment, and derive an empirical formula for the peak quasistatic pressure of a cabin explosion in a typical water mist environment. The main components of this paper are as follows: Section 2 focuses mainly on cabin explosion experiments in a water mist environment; Section 3 focuses mainly on the quasistatic pressure load characterization of confined cabins; and Section 4 focuses mainly on the further construction of the theoretical model of quasistatic pressure.

2. Cabin Explosion Experiments in a Water Mist Environment

2.1. Experimental Setup

The test model is a closed box-type cabin with geometric dimensions of 1 m \times 0.75 m \times 0.7 m and an interior volume of 0.525 m³, as shown in Figure 1. The cabin model material is made of Q235 steel with a plate thickness of 20 mm. It is equipped with reinforcement bars in both the longitudinal and transverse directions on the outside to ensure that the cabin does not deform under certain internal explosion conditions. To achieve cabin implosion in a water spray environment, a water spray system was used. The water mist system consists of a water pump with a water tank, high-pressure water pipes, and nozzles. The specific location of the water mist nozzle installation on the left and right sides of the cabin model is shown in Figure 2. In the XSW-T nozzle model, the flow coefficient is K = 0.15 [L/min/(MPa)^{1/2}], the nozzle operating pressure is between 4 and 10 MPa, and the theoretical flow rate can be computed as

$$Q = K\sqrt{10P_w} \tag{1}$$

where P_w is the pressure of the spray (MPa). The quasistatic pressure measurement uses a KD-YZ-40 sensor with a sampling frequency of 1 MHz and a range of 0–60 MPa, which contains a quasistatic test component that filters out the high-frequency shock wave component and performs a direct measurement of the low-frequency quasistatic pressure. The sensor is mounted externally to the bulkhead through the external threads of the front end and is symmetrically arranged at the front panel and the rear panel; its specific position is shown in Figure 3. The DH5960 dynamic signal acquisition system, which can collect dynamic data up to 1 MHz, was selected for quasistatic pressure data acquisition. The specific parameters of the TNT are shown in Table 1. For each test, the pillars were suspended in the center of the cabin, and the explosives were detonated using a detonator.

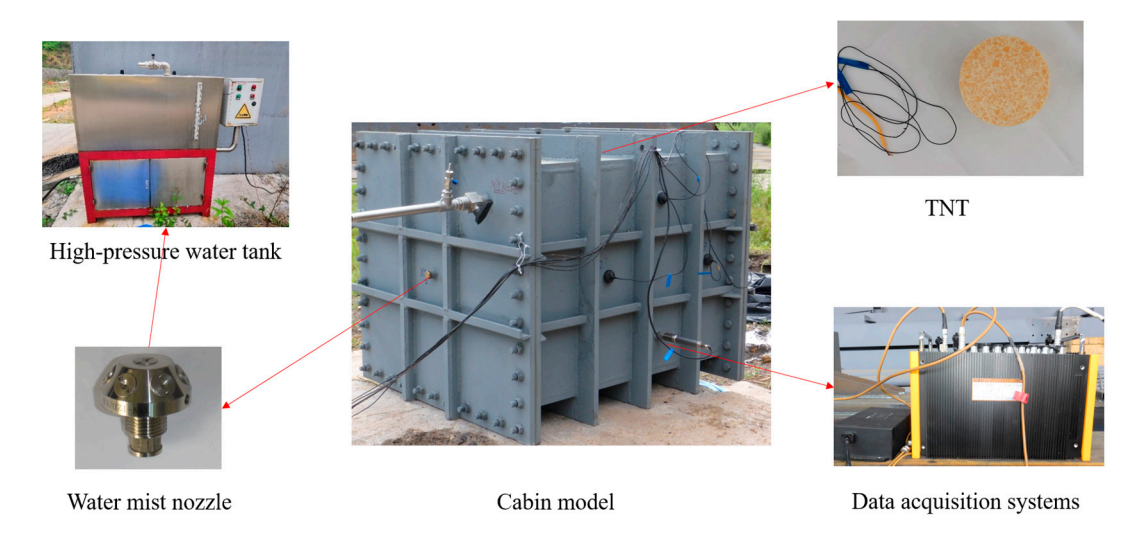


Figure 1. Integral test system for explosions in compartments under water spray environments.

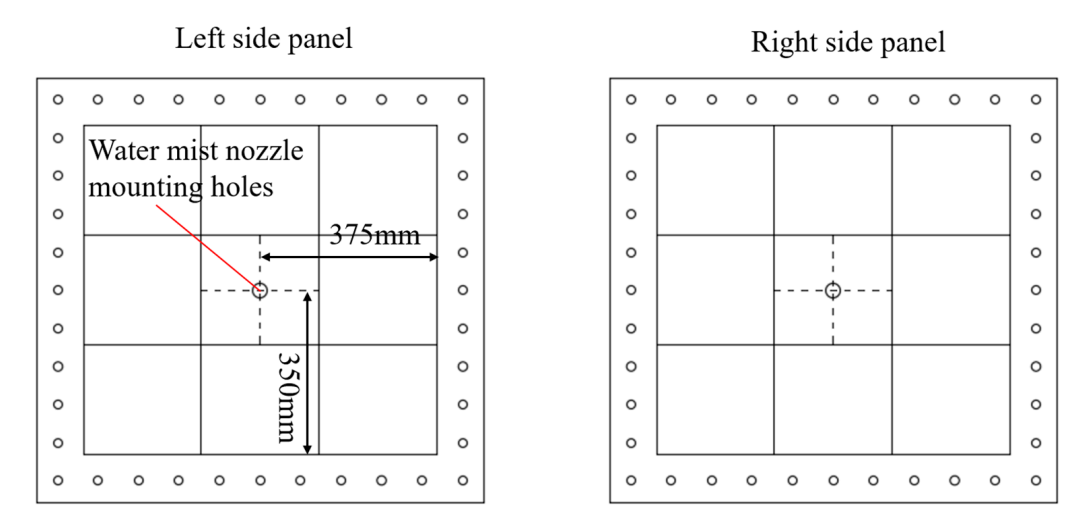


Figure 2. The specific location of the water mist nozzle installation.

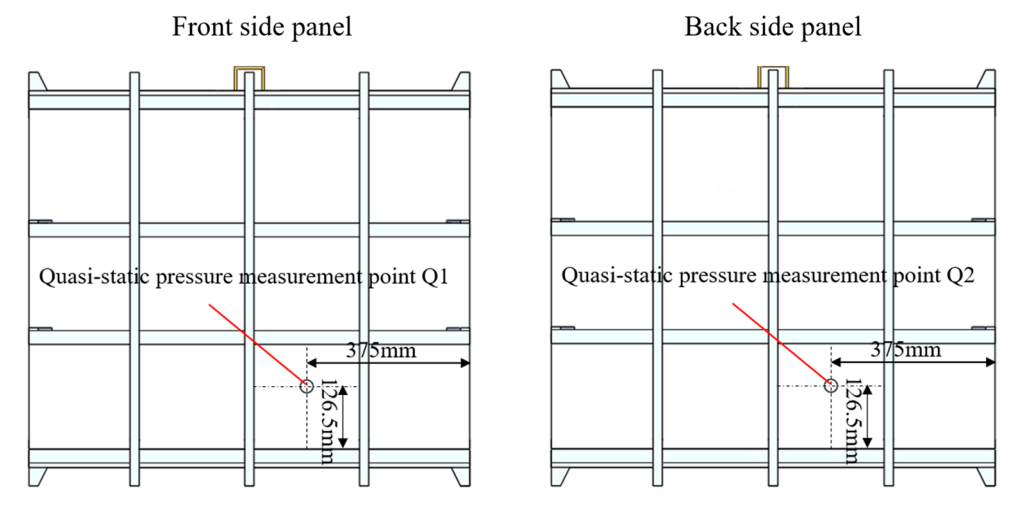


Figure 3. The specific layout of the quasistatic pressure measurement points.

Table 1. TNT charge-specific parameters.

Charge Density (g/cm³)	Charge Mass (g)	Charge Size (mm)
	7.8	Φ 25 × 10
1.633	12.5	$\Phi 30 \times 11$
	50	Φ 35.5 $ imes$ 32
	150	$\Phi 50 imes 48$
	250	$\Phi60 imes56$

2.2. Experimental Conditions and Parameter Measurements

To study the quasistatic pressure variation law of explosions in cabins with different explosive amounts and cabin volume ratios as well as water mist environments, the mass of the explosives and the concentration of water mist were considered the main variables in the design of the test conditions. Different water mist concentrations can be achieved by adjusting the water pressure. In addition, tests of a completely sealed cabin and an open cabin were conducted by closing and opening the sealing cover on the upper part of the cabin model. The test conditions are shown in Table 2. In the completely sealed cabin, five different explosive volumes, respectively, in the absence of a water spray environment and in the same water spray environment (with a 10 MPa water spray pressure), were tested five times in the cabin explosion test, e.g., Conditions 1–10, to study the same water spray environment, different explosive ratios, and the cabin explosion quasistatic pressure variation rule. To study the same explosive ratio, different water spray environments were used in the cabin explosion quasistatic pressure variation rule, and Conditions 11–16 were designed.

Table 2. Experimental working conditions.

Condition No.	Charge Mass (g)	Water Spray Pressure (MPa)	Temperature (°C)	Humidity %
1	7.8	-	24.6	53.1
2	12.5	-	25.1	96.6
3	50	-	23.8	61.7
4	150	-	30.3	53.1
5	250	-	29.6	91.6
6	7.8	10	24.3	94.2
7	12.5	10	27.9	95.2
8	50	10	28.7	97.3
9	150	10	30.0	92.3
10	250	10	25.6	75.9
11	50	4	26.5	95.8
12	50	6	25.1	91.6
13	50	8	23.6	96.9
14	150	4	26.4	87.3
15	150	6	24.2	94.2
16	150	8	25.6	98.3

For a fully confined cabin without water spray explosion conditions (Conditions 1–5), the test process involves the following steps: First, a quasistatic pressure sensor was installed in the corresponding position of the cabin model, with the bolt plugging the water spray nozzle's mounting holes. The TNT was then hung to a predetermined position, the sealing cap was installed, the data acquisition system was calibrated and turned on, and the detonation of the TNT occurred 15 s after the end of the data acquisition process. A completely confined cabin with water spray explosion conditions (Conditions 6–16) was used as follows: the water spray nozzle was installed, the water pressure was adjusted to the corresponding value, the TNT was hung to a predetermined position, the sealing cover was installed, the water spray switch was opened, and the time used was 30 s, which ensured the formation of a roughly uniform

field of fog in the cabin. The data acquisition system was subsequently calibrated and turned on, the TNT was detonated, and data acquisition was terminated after 15 s.

The quasistatic pressure of an explosion in a cabin in a water mist environment is closely related to the ratio of the amount of charge to the cabin volume, and different water mist environments affect the test results similarly. Therefore, the water mist concentration and droplet diameter were measured for the water mist environment under these test conditions. Moreover, the water mist sprayed in the space for a period of time forms a uniform fog field in the cabin space. A large number of droplets fall to the bottom of the cabin due to gravity, forming larger droplets that do not participate in the explosion process inside the cabin. In the explosion process, water mist participates in the explosion instant residual in the space as small droplets. Therefore, the water mist concentration was measured via the weighing method, as shown in Figure 4. A transparent acrylic plate was used to construct a model with the same geometric dimensions as the cabin model in the explosion test. At the bottom of the model, four tension and pressure sensors were used to lift a water collection tray, which has an area slightly larger than the bottom area of the model. The nozzle was installed at the position corresponding to the explosion cabin, and spraying was started and continued for 1 min. Data from the tension and compression sensors were collected to obtain the growth curve of the mass of the drop falling to the bottom of the cabin with time. The mass corresponding to a certain time t after the slope was stable was recorded as m_1 . In addition, the growth curve of the water mist mass at the outlet of the two water mist nozzles was measured over time, and the mass corresponding to the same time t was recorded as m_2 . The difference between the two methods is the mass of water mist remaining in the space; then, the water mist concentration ρ_w can be expressed as

$$\rho_w = \frac{m_2 - m_1}{V} \tag{2}$$

where *V* represents the volume of the cabin. The measured water mist concentrations at different water spray pressures are shown in Table 3.

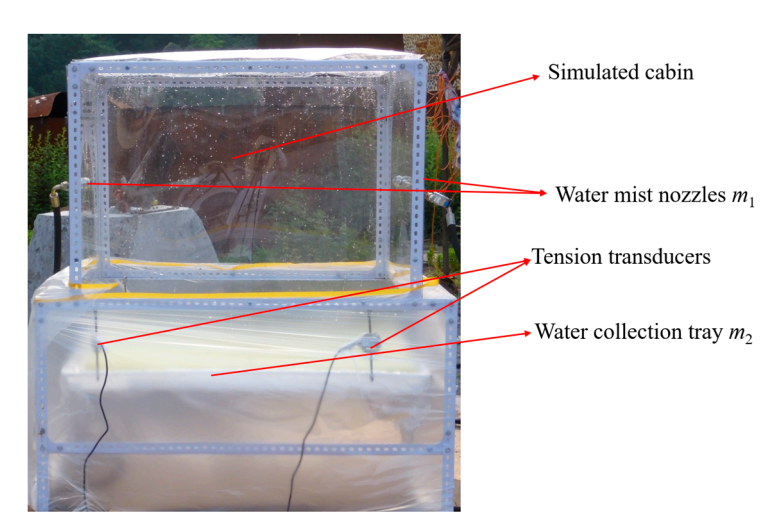


Figure 4. Water mist concentration measuring device.

Table 3. Water mist concentrations at different spray pressures (the water mist concentrations in the table are characteristic concentrations).

Flow Coefficient K	Water Spray Pressure (MPa)	Water Mist Concentration (g/m³)
0.15	4	0.087
	6	0.105
	8	0.115
	10	0.123

Previous studies have shown that the diameter of water mist droplets affects the explosion pressure [18]; therefore, droplet size measurements were carried out for water mist spraying conditions under these test conditions. The droplet diameter and fog field distribution during the Winner319B spray laser particle sizer are shown in Figure 5. The test results were provided by the Beijing Zhongke Institute of Optical Analysis Science and Technology. The average particle sizes of the droplets under different water spray pressures are shown in Table 4.

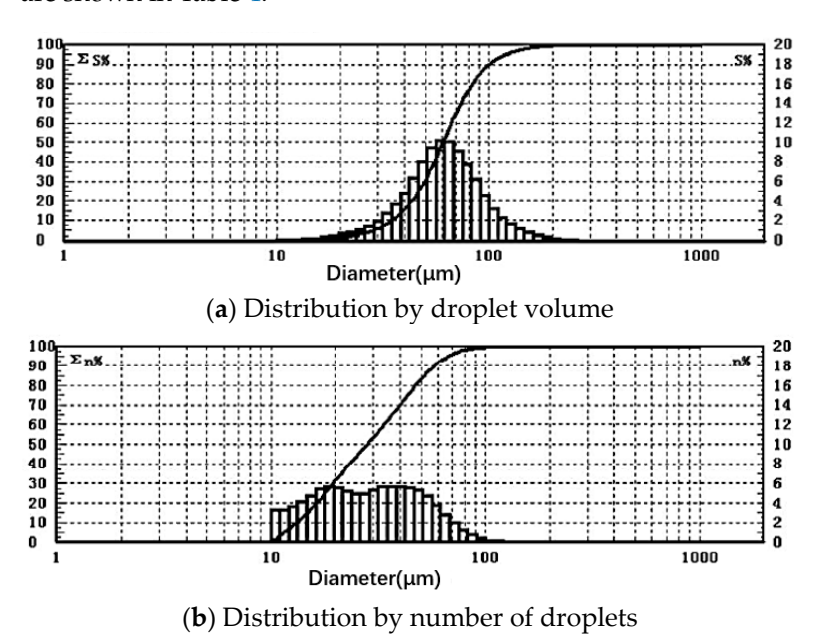


Figure 5. Water mist particle size distribution curve (K = 0.15; P = 4 MPa).

Table 4. Droplet sizes at different water spray pressures.

Flow Coefficient K	Water Spray Pressure (MPa)	Average Droplet Diameter (μm)
0.15	4	59.343
	6	55.545
	8	55.877
	10	51.399

2.3. Experimental Results

As shown in Figure 6, the quasistatic pressure at the Q1 measurement point was measured during the explosion of 12.5 g of TNT in a completely sealed cabin without and with water mist under Conditions 2 and 7, respectively. The pressure variation inside the cabin can be divided into three stages: the shock wave pressure reaches its peak within 2 ms and rapidly decreases; the air pressure increases at approximately 2–20 ms; and the pressure reaches a relatively stable quasistatic state within 20–80 ms and slowly decreases. The air pressure increases because the temperature of the gas inside the cabin increases because of the combustion of explosive products. The pressure rebound is significant in the presence of water mist and takes longer than in the absence of water mist, and the peak quasistatic pressure is significantly delayed. This may be due to the presence of water mist reducing the intensity of post-combustion reactions. After the peak quasistatic pressure is reached, the overall quasistatic pressure tends to stabilize, indicating a quasistatic platform effect. In the subsequent discussion of the quasistatic pressure in a completely confined cabin, the quasistatic pressure peak can be applied to characterize the explosion quasistatic pressure. The test results for all working conditions in the confined cabin are shown in Table 5. When the dosage is between 7.8 and 250 g and the water mist concentration is between 0.087 and 0.123 kg/m³, when the quasistatic pressure load of the cabin explosion

in the presence and absence of water mist is compared, the attenuation of the quasistatic pressure peak is between 9.66 and 43.73%, and the attenuation rate of the arrival time of the quasistatic pressure peak is between 50.00 and 72.73%. The results indicate that water mist has a significant weakening effect on the quasistatic pressure peak and delays the arrival time of the quasistatic pressure peak.

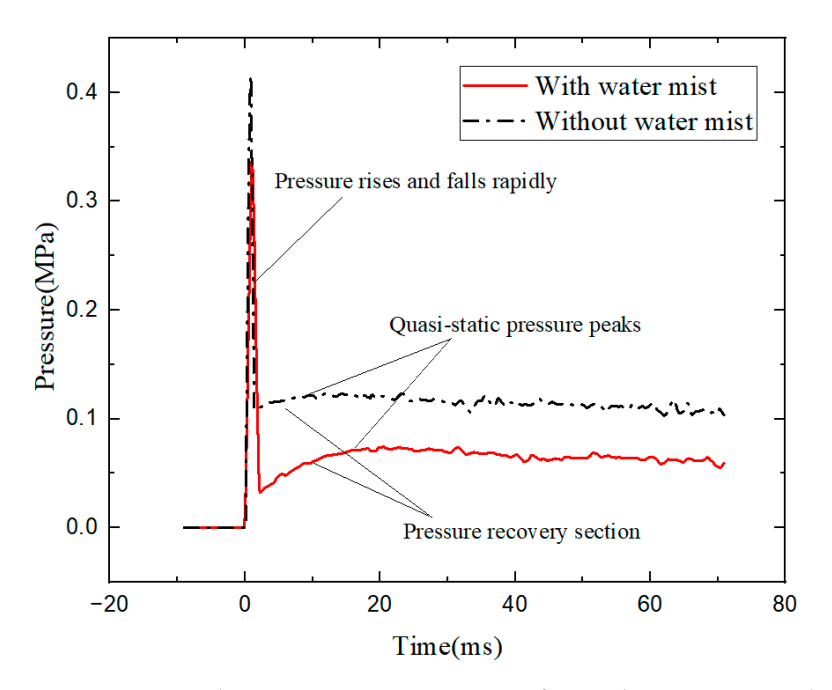


Figure 6. Typical quasistatic pressure curves for implosion in a completely sealed cabin in an environment with and without water spray.

Table 5. Experimental results for sealed cabin.

Condition	Charge Mass (g)	Water Spray Concentration (kg/m³)	Quasistatic Pressure Peak (MPa)	Quasistatic Pressure Peak Weakening Rate	Quasistatic Pressure Peak Arrival Time (ms)	Rate of Delay in Arrival Time
1	7.8		0.080	-	13	-
2	12.5		0.121	-	12	-
3	50	-	0.295	-	12	-
4	150		0.621	-	11	-
5	250		0.878	-	11	-
6	7.8		0.057	28.75%	21	61.54%
7	12.5		0.072	40.50%	20	66.67%
8	50	0.123	0.166	43.73%	18	50.00%
9	150		0.436	29.79%	18	63.64%
10	250		0.684	22.10%	18	63.64%
11	50	0.087	0.228	22.71%	18	50.00%
12	50	0.105	0.201	31.86%	19	58.33%
13	50	0.115	0.177	40.00%	19	58.33%
14	150	0.087	0.561	9.66%	18	63.64%
15	150	0.105	0.501	19.32%	19	72.73%
16	150	0.115	0.457	26.41%	19	72.73%

3. The Quasistatic Pressure Load Characterization of the Confined Cabin

3.1. Quasistatic Pressure Theory Modeling

To further construct the theoretical model of quasistatic pressure, two assumptions are introduced on the basis of the model of the ideal gas internal explosion [19]: (1) the

water mist is completely evaporated at the instant of explosion and (2) the energy loss is ignored. The energy generated by the explosion is completely used to provide the latent heat of evaporation of the water mist and to heat the gas in the cabin, thus establishing a theoretical model of the quasistatic pressure of the implosion in the water mist environment. After the detonation of explosives in a sealed cabin, as time increases, the amplitude of and fluctuation in the explosion pressure weaken, and the gas pressure of the detonation products is evenly distributed in the sealed space, producing a pressure amplitude much smaller than the initial reflected impact load peak but with a long duration (usually tens of milliseconds), that is, quasistatic pressure. Small-diameter droplets are sprayed into the cabin before the explosion, and after a period of time, the droplets form a uniform mist field inside the cabin and then detonate the explosive. This is a cabin explosion in a fine water mist environment. Salter et al. [20] reported that the droplets in a cabin fog field have a very large surface area, providing an excellent opportunity for droplet evaporation. Most of the heat generated by the explosion can be transferred to the droplets in a few milliseconds. Willauer et al. [11] reported that the evaporation time required for a droplet with a diameter of 51 µm is 60 ms when an explosion occurs in a closed environment. According to the quasistatic pressure curve measured by Kong et al. [10] in a water mist environment, approximately 15 ms after the explosion, the cabin pressure tends to be quasistatic, and then the quasistatic pressure continues until 50 ms. Based on the above study, the time required for droplet evaporation is longer than the time required for quasistatic pressure to be generated and sustained in practical situations, and the two pressures do not occur simultaneously at the moment of explosion. However, their magnitudes are both in the tens of milliseconds range, which is still a fast process. Therefore, it can be assumed that the water mist completely evaporates at the moment of explosion when a theoretical model of the quasistatic pressure of implosion in a water mist environment is established. Under the assumption that the explosion product is an ideal adiabatic gas model, the quasistatic pressure can be divided into two parts: (1) when the temperature is constant, the cold pressure state is caused by the explosion gas product and water vapor in a closed space, and (2) the energy generated by the explosion causes the rapid evaporation of water mist and variations in the temperature of the gas inside the cabin, resulting in a hot pressure state caused by pressure variations. Dalton's law of partial pressure can be expressed as

$$p_1 = p_0 \frac{mV_0 + m_w V_e}{V} (3)$$

where p_0 is the cabin's initial pressure; m is the mass of the explosives; V_0 is the specific volume of explosion; V is the cabin's volume; m_w is the mass of the water spray; and V_e is the specific volume of water vapor.

The response of liquid droplets in the implosion of a closed cabin in a water mist environment is very complex, and in general, the explosion shock wave energy is mainly converted into the following forms: (1) droplet kinetic energy; (2) droplet surface energy; (3) droplet sensible heat of vaporization; (4) droplet latent heat of vaporization; and (5) gas sensible heat heating [21]. Adiga et al. [22] reported that the fragmentation of a 0.5 mm diameter droplet into 10,000 droplets with a diameter of 23 μ m requires a very small increase in the fragmentation energy of 18 J/kg per unit mass compared with 2.25 \times 106 J/kg per unit mass. Ananth et al. [16] and Thomas et al. [23] used numerical simulations and experimental studies, respectively, to obtain a common conclusion: compared with water mist evaporation sensible heat and droplet motion, the explosion energy is converted into the vast majority of the latent heat of evaporation of water mist. Therefore, we do not consider the kinetic energy of the droplets, surface energy, or evaporation of sensible heat. Assuming that the energy loss is ignored, the explosion energy is completely used to provide the latent heat of evaporation of water mist and the heat of the gas in the cabin as follows:

$$mq = m_{g}C_{V}\Delta T + m_{w}L_{a} \tag{4}$$

where q is the heat during the explosion of the explosives; m_g is the mass of gas in the cabin; C_V is the specific heat of the gas constant volume; ΔT is the temperature variation in the cabin; and L_a is the latent heat of evaporation per unit mass of water spray.

From the ideal gas equation of state, the pressure can be expressed as

$$p_2 = \rho_g R \Delta T = \rho_g R \frac{mq - m_w L_a}{m_g C_V} \tag{5}$$

$$C_V = \frac{R}{\gamma - 1} \tag{6}$$

where ρ_g is the gas density; R is the ideal gas constant; and γ is the gas-specific heat ratio. The theoretical formula for the quasistatic pressure peak in a water mist environment is given as follows:

$$P_{qs,\text{max}} = p_1 + p_2 = p_0 \left(\frac{m}{V} V_0 + \frac{m_w}{V} V_e \right) + (\gamma - 1) \left(\frac{m}{V} q - \frac{m_w}{V} L_a \right)$$
 (7)

The above theoretical derivation is based on a variety of assumptions. Owing to the involvement of water spray in the reaction between the explosion products and air, resulting in a very complex after-burning process, the theoretical calculations inevitably have a large discrepancy with the experimental measurements. However, as seen from the above equation, the peak quasistatic pressure of cabin implosion in a fine water mist environment is closely related not only to the charge/volume ratio but also to the water mist mass/volume ratio, i.e., the water mist concentration.

$$P_{qs,\max} = f\left(\frac{m}{V}, \frac{m_w}{V}\right) \tag{8}$$

3.2. Empirical Equations for the Quasistatic Pressure Based on Experimental Data

When the water mist concentration is approximated, i.e., when the approximation is considered constant, the following equation can be considered:

$$P_{qs,\max} = f\left(\frac{m}{V}\right) \tag{9}$$

Conditions 1–10 in Table 5 are comparable in environments without and with water mist, and the measured quasistatic pressure peaks are shown in Table 6. The test results of the quasistatic pressure peaks without and with water mist and their fitting curves are shown in Figure 7.

Table 6. Conditions 1–10. Quasistatic pressure peaks with and without water mist (note: quasistatic pressure peaks in this table are all gauge pressures).

V/m³ m/kg		m/kg $(m/V)/$ (kg/m^3)	Water Spray Concentration	pcs, max/MPa		Result of Subtraction/MPa
		(kg/m²)	$/(g/m^3)$	Waterless Mist	Misty	
0.525	0.0078	0.015	123	0.080	0.057	0.023
0.525	0.0125	0.024	123	0.121	0.072	0.049
0.525	0.05	0.095	123	0.295	0.166	0.129
0.525	0.15	0.286	123	0.621	0.436	0.185
0.525	0.25	0.476	123	0.878	0.684	0.194

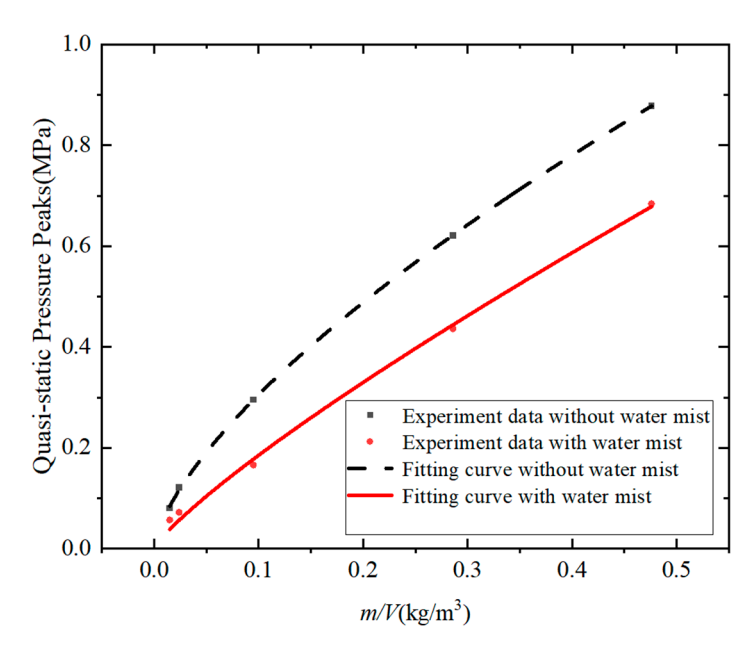


Figure 7. Quasistatic pressure peaks in environment with and without water mist vs. fitted curves.

As shown in Figure 7, in an environment in the absence and presence of water mist, the peak quasistatic pressure of TNT implosion increases nonlinearly with an increasing m/V value. According to Equation (9), the test data are fitted to the form of a power function of m/V, and the empirical equation of the peak quasistatic pressure can be obtained as follows: For waterless mist:

$$p_{qs,\text{max}} = (1.450 \pm 0.011) \left(\frac{m}{V}\right)^{0.676}$$
 (10)

For a water mist environment:

$$p_{qsw,\text{max}} = (1.251 \pm 0.060) \left(\frac{m}{V}\right)^{0.785} \tag{11}$$

A comparison of the calculated results of Equation (11) with the test values reveals that the overall deviation between the quasistatic pressure peak calculated according to Equation (11) and the experimental quasistatic pressure peak is less than 20%, as shown in Table 7. Within the applicable range, the equation can be used for quickly calculating the quasistatic pressure peak of internal explosions in water mist environments.

Table 7. A comparison of the calculated results using Equation (11) with the experimental values.

$(m/V)/(kg/m^3)$	Experimental Value/MPa	Calculated Value/MPa	Deviation
0.015	0.057	0.046	18.79%
0.024	0.072	0.067	7.02%
0.095	0.166	0.197	-18.76%
0.286	0.436	0.468	-7.40%
0.476	0.684	0.699	-2.12%

When the dose/volume ratio m/V is constant, i.e., m/V is considered to be constant, it can be assumed that

$$p_{qs} = f\left(\frac{m_w}{V}\right) \tag{12}$$

Conditions 8, 9, and 11–12 in Table 5 are the internal explosion tests of 50 g and 150 g of TNT at different water mist concentrations. The peak quasistatic pressures measured under different water mist concentrations in the experiment are shown in Table 8. The

experimental results and fitting curves of the quasistatic pressure peak values of the 50 g and 150 g dosages at different water mist concentrations are shown in Figure 8.

Table 8. Experimental values of quasistatic pressure peaks at different water mist concentrations (the
quasistatic pressure peaks in the table are the gauge pressures).

V/m ³	m/g	(<i>m</i> /V)/(kg/m ³)	Flow Coefficient K	Water Spray Pressure (MPa)	m _w /V/ (kg/m ³)	$P_{qs,\mathrm{max}}/\mathrm{MPa}$
0.525	50	0.095	0.15	4	0.087	0.228
0.525	50	0.095	0.15	6	0.105	0.201
0.525	50	0.095	0.15	8	0.115	0.177
0.525	50	0.095	0.15	10	0.123	0.166
0.525	150	0.286	0.15	4	0.087	0.561
0.525	150	0.286	0.15	6	0.105	0.501
0.525	150	0.286	0.15	8	0.115	0.457
0.525	150	0.286	0.15	10	0.123	0.436

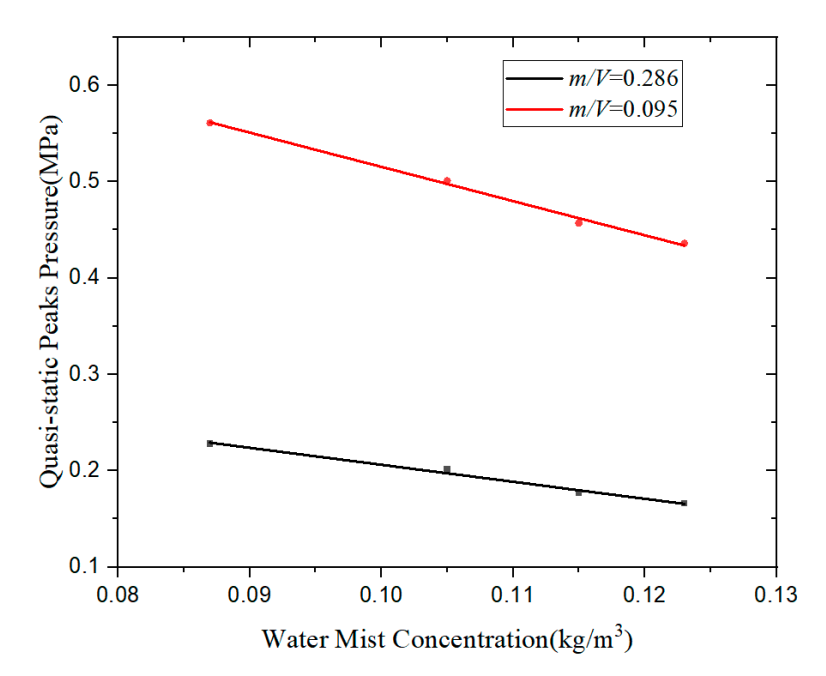


Figure 8. Peak quasistatic pressure vs. fitted curves at different water mist concentrations for 50 g and 150 g charge masses (the dots are corresponding to the quasistatic pressure peaks at different water mist concentrations).

As shown in Figures 4–6, the quasistatic pressure peak of the TNT implosion with an increasing m_w/V value decreases approximately linearly at m/V=0.095 and m/V=0.286, which indicates that increasing the concentration of the water spray can effectively reduce the quasistatic pressure peak in the range of $0.087~({\rm kg/m^3}) \le m_w/V \le 0.123~({\rm kg/m^3})$. According to Equation (12), the test data are fitted to the form of a linear function of m_w/V , which can be obtained from m/V=0.095 and m/V=0.286. The empirical equation of the peak quasistatic pressure is given as follows:

$$p_{qs,\text{max}} = -1.765 \frac{m_w}{V} + 0.383, m/V = 0.095$$
 (13)

$$p_{qs,\text{max}} = -3.551 \frac{m_w}{V} + 0.871, m/V = 0.286$$
 (14)

The range of application of the two equations is $0.087 \, (\text{kg/m}^3) \leq m_w/V \leq 0.123 \, (\text{kg/m}^3)$. It was concluded above that the quasistatic pressure of an implosion in a fully confined cabin in a water mist environment is closely related to the charge/volume ratio m/V and the water mist concentration m_w/V . Equation (7) shows that the effects of m/V and m_w/V on the quasistatic pressure, pcs, are independent of each other.

As shown in the previous two sections, when the water spray concentration is constant, the peak quasistatic pressure of a TNT implosion with an increasing m/V value shows a nonlinear increase in the peak quasistatic pressure, which can be expressed as a power function in the form of m/V. When the charge/volume ratio does not vary, the peak quasistatic pressure with an increasing m_w/V value approximately linearly decreases, and the peak quasistatic pressure can be expressed as a linear function of m_w/V . Therefore, the quasistatic pressure equation for variations in both the charge/volume ratio and the water mist concentration can be expressed as

$$p_{qs,\text{max}} = k_1 \left(\frac{m}{V}\right)^{\alpha} + k_2 \frac{m_w}{V} + \beta \tag{15}$$

The experimental data of the quasistatic peak pressure of a cabin explosion under the different conditions measured in Table 5 are substituted into Equation (15) to obtain a nonlinear equation system. The numerical solution for the four coefficients k_1 , k_2 , α , and β can be expressed as the empirical formula for the quasistatic pressure of a completely confined cabin explosion in a water mist environment, which is given by

$$p_{qs,\text{max}} = 1.242 \left(\frac{m}{V}\right)^{0.86} - 2.615 \frac{m_w}{V} + 0.335 \tag{16}$$

Equation (16) is applied to the following:

$$0.015 (kg/m^3) \le m/V \le 0.476 (kg/m^3), \ 0.087 (kg/m^3) \le m_w/V \le 0.123 (kg/m^3)$$
 (17)

The experimental data of the quasistatic pressure peak value of the cabin explosion in the water mist environment are substituted from Table 5 into Equation (16). A comparison between the calculated peak quasistatic pressure and the experimental values is shown in Table 9. Under different explosive volume ratios (m/V) and water mist concentrations (m_w/V), the deviation between the calculated peak quasistatic pressure and the experimental values is less than 20%. Therefore, within the applicable range, Equation (16) can be used to quickly calculate the peak quasistatic pressure of internal explosions in water mist environments.

Table 9. A comparison of the theoretical and experimental values under quasistatic pressure.

(m/V)/(kg/m ³)	$m_w/V/(g/m^3)$	Experimental Value (MPa)	Calculation of Equations (2)–(17) (MPa)	Misalignment %
0.095	0.087	0.228	0.272	-19.10%
0.095	0.105	0.201	0.224	-11.68%
0.095	0.115	0.177	0.198	-12.05%
0.095	0.123	0.166	0.177	-6.87%
0.286	0.087	0.561	0.531	5.39%
0.286	0.105	0.501	0.484	3.46%
0.286	0.115	0.457	0.458	-0.11%
0.286	0.123	0.436	0.437	-0.14%
0.015	0.123	0.055	0.047	14.74%
0.024	0.123	0.076	0.064	16.31%
0.476	0.123	0.634	0.669	-5.57%

4. An Expansion of the Applicability of Empirical Formulas Based on a Numerical Simulation

4.1. Numerical Simulation Method and Validation

The mathematical model of an explosion in a cabin in a water mist environment is a type of two-component, two-phase flow. In this model, the TNT explosion utilizes the instantaneous detonation model, which can be simplified into an explosive gas mass as the gas phase in the two-phase flow. Fine water mist, which is the liquid phase in two-phase flow, is sprayed into micrometer-sized droplets inside the cabin. However, owing to the evaporation of droplets during interactions with the gas phase, the mass transport of the liquid phase to the gas phase needs to be considered. Therefore, the gas phase is a mixture of air and water vapor. The gas phase is considered a continuous phase, and the liquid phase is a discrete phase. In Ansys/Fluent 2019, discrete-phase droplets are simulated via the DPM model [16], and the breaking effect of water mist droplets is described via the TAB (Taylor Analogy Breakup) breaking model. The continuous phase of the explosive air mass is calculated by discretely solving the Reynolds-averaged compressible N–S equation via the finite volume method; the discrete phase of the water mist particles is solved via the Lagrangian tracking technique to determine the state of the water mist particles. As the breakage, motion, and evaporation of droplets are considered, there is an interaction between the two phases; therefore, two-way coupling is used in the calculation. On the basis of the above numerical simulation ideas, the simulation method of a cabin explosion in a water mist environment includes the following steps:

1. A calculation domain geometric model of the cabin explosion flow field is created, boundary conditions are set, and the geometric model is meshed. 2. The MATLAB program is used to generate the water mist information file, which is imported into the Ansys/Fluent 2019 software. Water mist information, including the coordinates of the droplets, velocity, particle size, temperature, mass, and other parameters, is used. 3. Two-way coupling conditions are set up according to the instantaneous blast model, which is filled with an explosive air mass. 4. The cabin explosion shock wave and water mist two-phase coupling are calculated to obtain the current time step of the flow field characteristics, which is based on the flow field characteristics of the explosion shock wave—water mist particle force. The deformation of the water mist particles, crushing and evaporation, and other processes are calculated, and the state of the water mist particles is updated. 5. According to the state of the water mist particles in the flow field due to the reaction of the source terms is calculated according to the reaction source term to update the two-phase coupling of the N–S equation to obtain the new explosion shock continuous-phase flow field. The overall simulation process is illustrated in Figure 9.

Owing to the short duration of TNT detonation, it can be assumed that the explosion is completed instantaneously, generating high-temperature and high-pressure explosion products. Therefore, as long as the TNT blast pressure and temperature are calculated via the Ansys/Fluent 2019 software, which assumes the presence of high-temperature and high-pressure gas, two-way coupling calculations can be subsequently performed to simulate the explosion shock wave. However, owing to the small volume of the charge masses used in the test, the number of grids filled is small, which can easily cause large errors in the calculation results. Therefore, owing to the conservation of mass and energy, cylindrical TNTs produced from high-temperature and high-pressure blast products are equivalent to a spherical shape and undergo a twofold increase in size. The calculated parameters of the gas cloud are shown in Table 10.

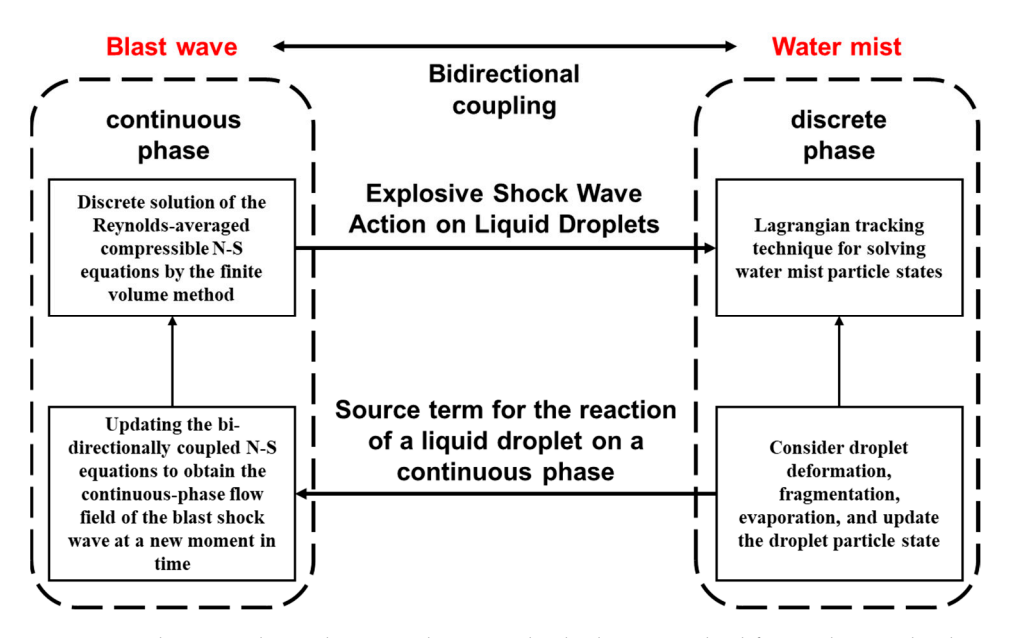


Figure 9. Bidirectional coupling simulation and calculation method for explosion shock wave and water mist droplet in cabin.

Table 10. Exploded air mass parameters.

Charge Mass (g)	Original Size (mm)	Two Times the Radius of a Sizeable Spherical Air Mass (mm)	Density (kg/m³)	Stress (Pa)	Temperature (K)
7.8	Φ 25 × 10	10.54	197.5	3.318×108	2782
12.5	$\Phi 30 \times 11$	12.29	197.5	3.318×108	2782
50	Φ 35.5 \times 32	19.63	197.5	3.318×108	2782
150	$\Phi 50 imes 48$	28.23	197.5	3.318×108	2782
250	$\Phi60 \times 56$	33.56	197.5	3.318×108	2782

The values of temperature in Table 10 are taken from the results of the research presented in reference [24]. It is assumed that the bulkhead is ideally rigid, so the boundary of the air domain in the cabin is set as a rigid wall. The air domain model is established with the center of the cabin as the origin, and its size is $1000~\text{mm} \times 750~\text{mm} \times 700~\text{mm}$. The boundary of the face in contact with the bulkhead is set as a rigid wall, and the pressure monitoring points are arranged at the corresponding positions of the test. The air domain grid cells are polyhedral, and the cell sizes are 6, 10, 16, and 24 mm from the center outward, as shown in Figure 10.

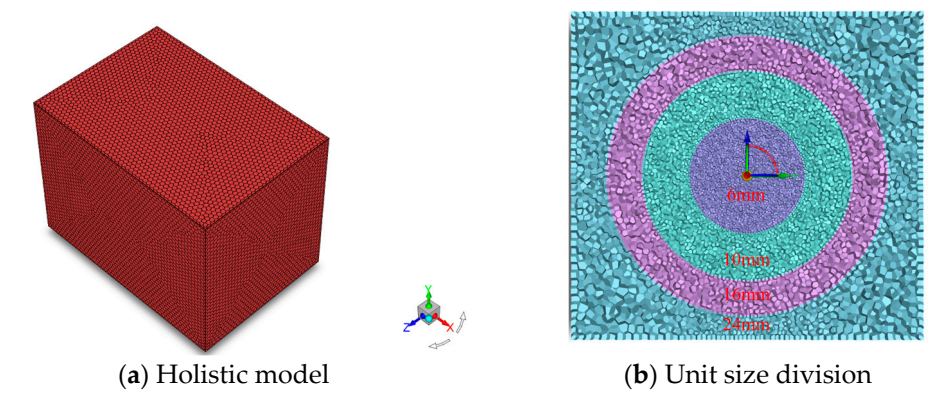


Figure 10. Simulation model of fully confined cabin.

In the simulation method, different water mist particle sizes, water mist concentrations, and initial water mist temperatures can be realized. The droplet shapes in the generated fog field are all spherical. Each droplet has the same diameter, thermal conductivity, and specific heat capacity. The temperature inside the droplet is uniformly distributed. The droplet diameter is based on the experimental measurement data, the droplet temperature is 300 K, the droplets are randomly distributed in the cabin and have no initial velocity, and the initial fog field is almost uniformly distributed throughout the cabin, as shown in Figure 11.

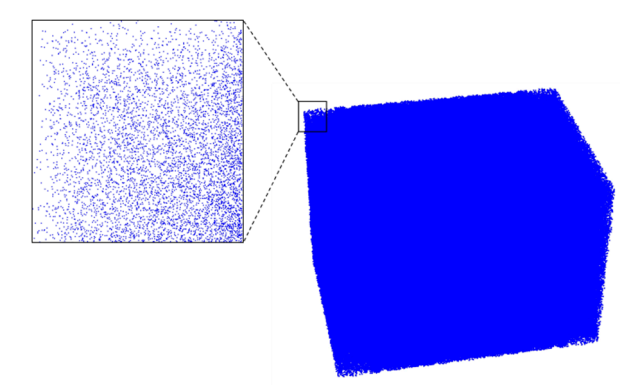


Figure 11. Initial fog field distribution.

A comparison between the simulation and experimental results of the implosion of a fully confined cabin in an environment with and without water mist is shown in Table 11. Overall, the quasistatic pressure deviation with and without water mist is less than 10%. The simulation method presented in this paper is effective in calculating the quasistatic loading of the implosion of a fully confined cabin in a water mist environment.

Table 11. A comparison of the simulation results with the experimental results under quasistat	ic
pressure.	

Water Spray Concentration (g/m ³)	Charge Mass (g)	Quasistatic Pressure Simulated Values (MPa)	Quasistatic Pressure Test Value (MPa)	Misalignment
	7.8	0.084	0.080	5.00%
	12.5	0.126	0.121	4.13%
-	50	0.311	0.295	5.42%
	150	0.641	0.621	3.22%
	250	0.917	0.878	4.44%
	7.8	0.059	0.057	3.51%
0.123	12.5	0.077	0.072	6.94%
	50	0.177	0.166	6.63%
	150	0.455	0.436	4.36%
	250	0.721	0.684	5.41%

4.2. Quasistatic Pressure Variation Law

Based on the cabin explosion tests using 50 g and 150 g of TNT with different water mist concentrations, the following conclusions were drawn: when m/V = 0.095 and m/V = 0.286, the peak quasistatic pressure decreases approximately linearly with an increasing m_w/V value, which indicates that increasing the water mist concentration can effectively reduce the peak quasistatic pressure within this range. To further expand the scope of application of the empirical formula, simulation calculation conditions for water mist concentrations greater than 0.123 (kg/m³) under 50 g and 150 g charge masses were set up in a completely

sealed cabin, as shown in Table 12. The pressure variation curves of the cabin with time under different conditions are shown in Figure 12.

Table 12. Table of simulated calculation conditions in fully confined	cabin.
--	--------

Charge Mass (g)	Charge-Volume Ratio m/V (kg/m³)	Water Mist Quality m_w (kg)	Water Spray Concentration m_w/V (kg/m ³)	Quasistatic Pressure (MPa)
50	0.095	0.07	0.133	0.164
		0.08	0.152	0.162
		0.10	0.190	0.159
		0.11	0.210	0.156
150	0.286	0.07	0.133	0.401
		0.08	0.152	0.368
		0.10	0.190	0.315
		0.11	0.210	0.261

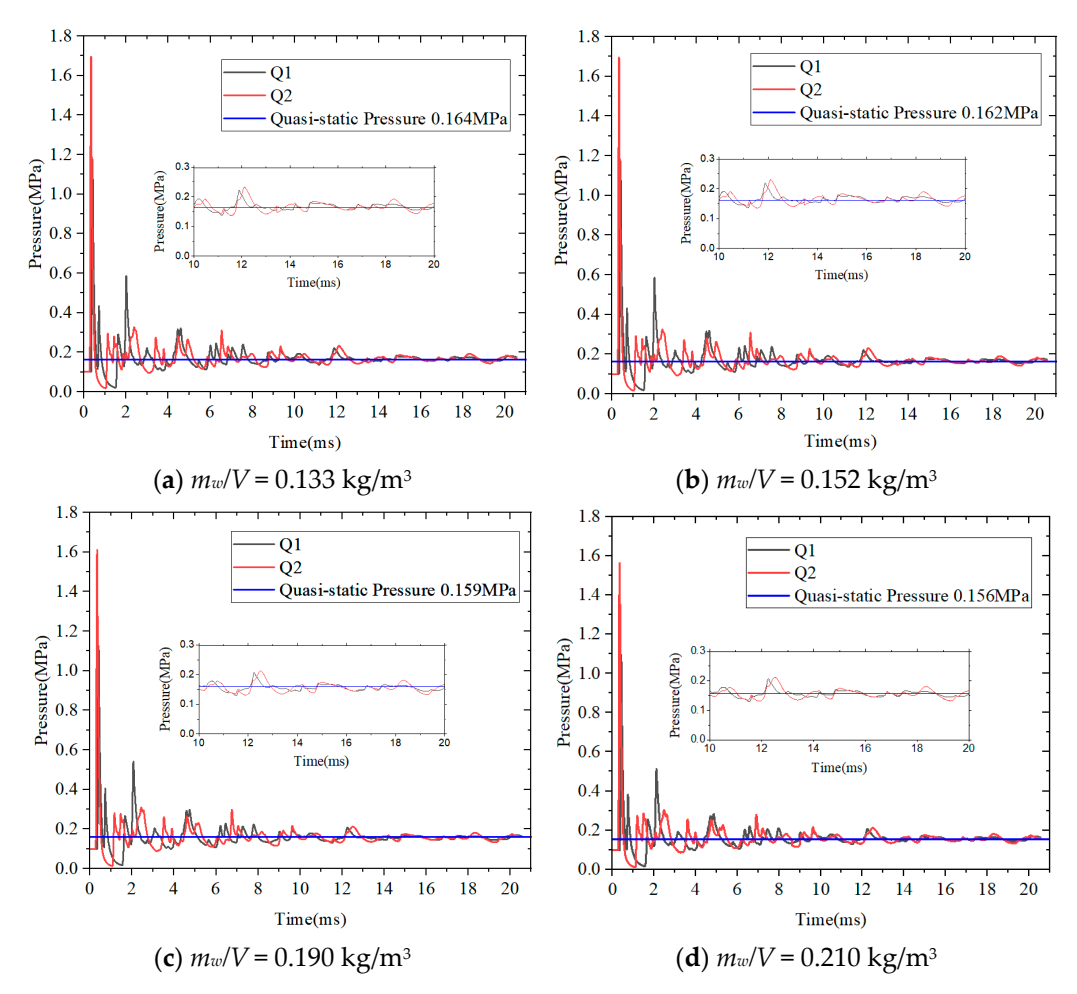


Figure 12. Quasistatic pressure curves for different water mist concentrations with 50 g charge mass.

As shown in Figures 12 and 13, the pressure of the explosion in the fully confined cabin at 0–1 ms rapidly increases and then stabilizes after 10 ms. Owing to the ideal completely sealed simulation model, there is no gas leakage. Due to the rigidity and insulation of the cabin walls, there are no significant fluctuations in pressure after they reach the quasistatic state. The simulation can be stopped after 20 ms. The quasistatic pressure is taken as the average pressure of measuring points Q1 and Q2 within 10–20 ms, as shown by the blue curve in Figures 12 and 13. According to Equation (16), the quasistatic pressures for

the simulated conditions are calculated and compared with the simulated data. Table 12 shows that for 50 g of TNT, the deviation between the empirical formula calculation results and the simulation results is relatively small at $m_w/V = 0.133$ (kg/m³). The empirical values are both smaller than the simulation values, and the deviation between the two is significant at $m_w/V > 0.133$ (kg/m³). However, the deviation between the empirical values and simulation values is within 20% under all simulation conditions with 150 g of TNT.

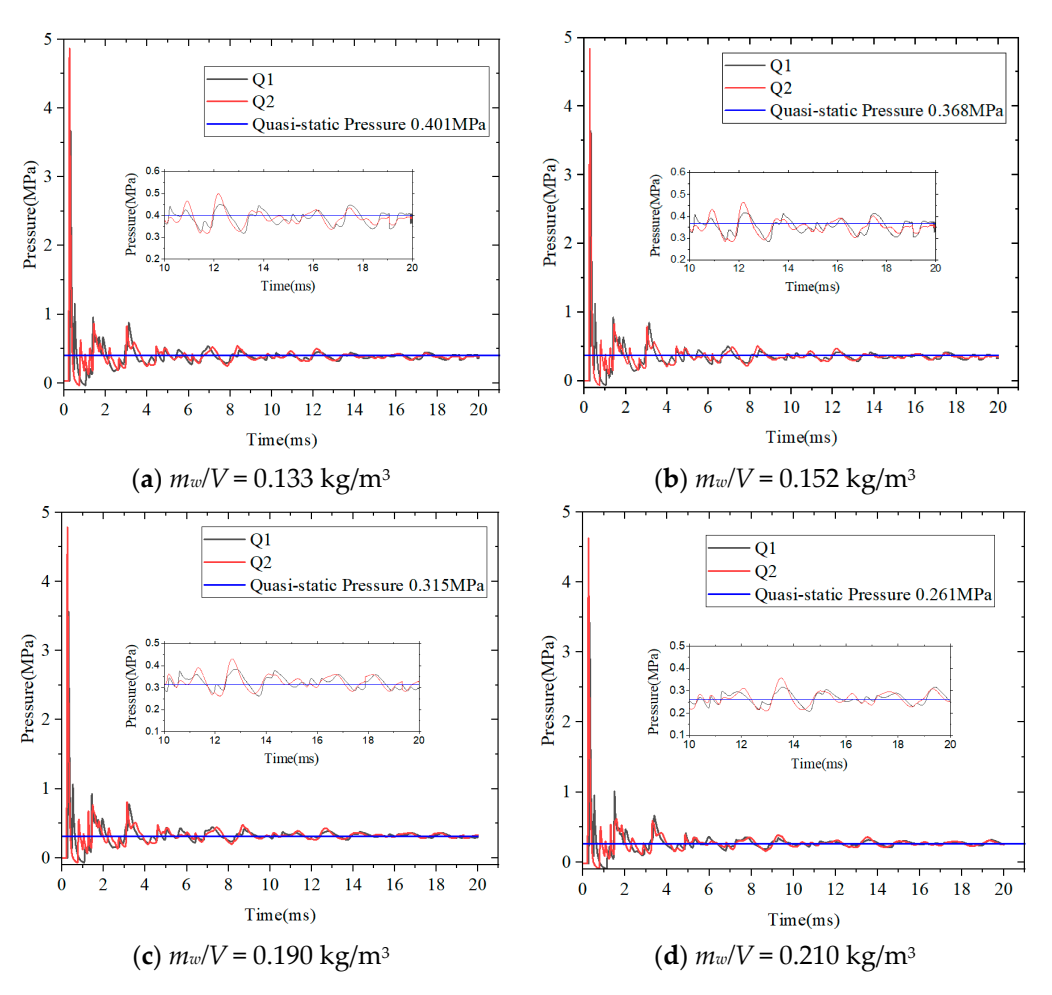


Figure 13. Quasistatic pressure curves for different water mist concentrations with 150 g charge mass.

A comparison between the experimental and simulation results of the quasistatic pressure with different water mist concentrations is shown in Figure 14. The quasistatic pressure still decreases approximately linearly with an increasing water mist concentration with 0.087 (kg/m³) < m_w/V < 0.210 (kg/m³) when the charge mass is 150 g. The slopes of the fitted straight lines are -2.27. When the charge mass is 50 g, i.e., 0.087 (kg/m³) < m_w/V < 0.133 (kg/m³), the quasistatic pressure decreases approximately linearly with an increasing water mist concentration, and the slope of the straight line is -1.50; however, when m_w/V > 0.133 (kg/m³), the quasistatic pressure, although similarly decreasing gradually, decreases very slowly, and the slope of the straight line is -0.10, which is only 0.95% of the first half. This suggests that the quasistatic pressure can be approximated as unvaried. The range of application of Equation 16 can be expanded to

$$0.015 (kg/m^3) \le m/V \le 0.476 (kg/m^3), 0.087 (kg/m^3) \le m_w/V \le 0.133 (kg/m^3)$$

$$\cap m/V = 0.286, 0.087 (kg/m^3), m_w/V \le 0.210 (kg/m^3)$$
(18)

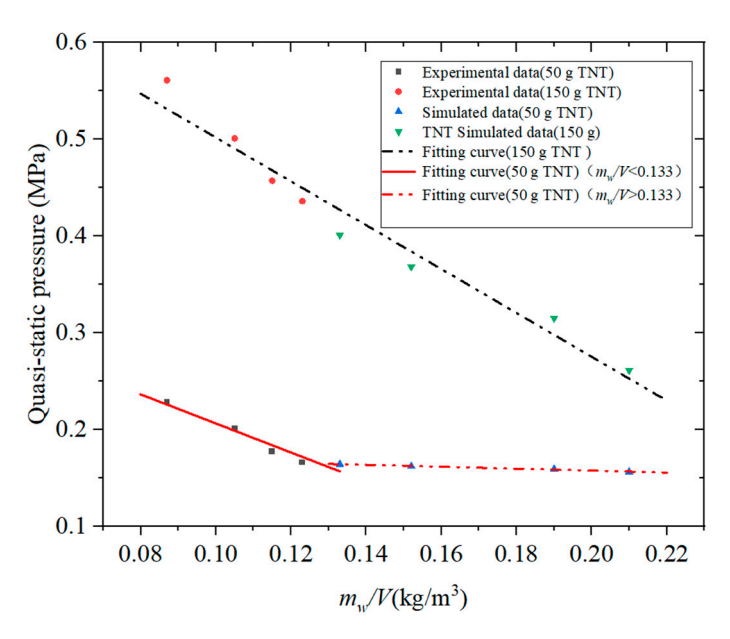


Figure 14. Quasistatic pressure for different water mist concentrations.

When m/V = 0.095 (kg/m³), the empirical formula can similarly be rewritten in segmented form, as Equation (19): And comparison of the calculated and simulated results of Equation (16) in a fully confined cabin is shown in Table 13.

$$\begin{cases}
 p_{qs,\text{max}} = 1.242 \left(\frac{m}{V}\right)^{0.86} - 2.615 \frac{m_w}{V} + 0.335 \text{ (MPa)}, \ 0.087 \text{ (kg/m}^3) \le m_w/V \le 0.133 \text{ (kg/m}^3) \\
 0.160 \text{ (MPa)}, \ m_w/V > 0.133 \text{ (kg/m}^3)
\end{cases}$$
(19)

Table 13. A comparison of the calculated and simulated results of Equation (16) in a fully confined cabin.

m/V (kg/m ³)	m_w (kg)	m_w/V (kg/m ³)	Equation (16) P_{qs} (MPa)	Simulation P_{qs} (MPa)	Misalignment
0.095	0.07	0.133	0.151	0.164	-7.77%
	0.08	0.152	0.102	0.162	-37.31%
	0.10	0.190	0.002	0.159	-98.62%
	0.11	0.210	-0.050	0.156	-132.12%
0.286	0.07	0.133	0.410	0.401	2.36%
	0.08	0.152	0.361	0.368	-1.96%
	0.10	0.190	0.261	0.315	-17.02%
	0.11	0.210	0.209	0.261	-19.89%

To verify the reliability of Equation (16), we compared the empirical formula with the experimental results in the literature [13], and the comparison results are shown in Table 14. The misalignments between the empirical formula and experimental results [9] are both within 10%. This shows that when the water mist concentration is less than the design concentration, Equation (19) similarly can be used to quickly estimate the quasi-static pressure in the water mist environment.

Table 14. A comparison of the empirical formula and experimental results [9].

<i>m/V</i> (kg/m ³)	Charge Type	m_w/V (kg/m ³)	Experiment P_{qs} (MPa)	Equation (19) P_{qs} (MPa)	Misalignment
0.1244	50 g TNT	0	0.510	0.542	6.20%
		0.070	0.331	0.359	8.43%
		0.057	0.365	0.393	7.50%

5. Conclusions

In this work, the quasistatic pressure load characteristics of explosions were investigated in a closed cabin under the influence of different explosive and water mist qualities. An explosion test in a confined cabin in a water mist environment was carried out, and a theoretical model of the quasistatic pressure during explosions in this environment was established. On the basis of the experimental data and theoretical models, an empirical formula for the peak quasistatic pressure of implosion in a water mist environment was proposed. The main conclusions are as follows:

- (1) A series of cabin implosion experiments in a water mist environment were conducted to obtain the quasistatic pressure inside the cabin. The test results show that when the quasistatic pressure loads of the cabin explosion in an environment with and without water mist were compared, the quasistatic pressure peak was reduced by 9.66% and 43.73%. Additionally, the arrival time of the quasistatic pressure peak was delayed in the range of 50.00% to 72.73%. These findings indicate that water mist has a significant weakening effect on the quasistatic pressure peak and delays the arrival time of the peak.
- (2) A theoretical model of quasistatic pressure for the implosion of a closed cabinet in a water mist environment was established. This model assumes that the water mist is completely evaporated at the moment of the explosion and that energy loss is negligible. Combined with the experimental data and theoretical model, an empirical formula for quasistatic pressure was proposed. This formula can be used in engineering to quickly calculate the quasistatic pressure peaks for implosions in a water mist environment.
- (3) A numerical simulation method for cabin implosion in a water mist environment was proposed, which further expands the scope of application of the empirical formulas.

Author Contributions: Methodology, X.L.; Software, Y.Z. (Ya Zhang); Validation, X.X.; Investigation, Y.Z. (Ya Zhang), X.X., H.H. and W.C.; Writing—original draft, Y.Z. (Ya Zhang) and W.C.; Writing—review & editing, M.L. and Y.Z. (Yiheng Zhang); Supervision, X.L. and W.C. All authors have read and agreed to the published version of the manuscript.

Funding: The research project was supported by the National Natural Science Foundation of China (grant numbers: 52201334).

Institutional Review Board Statement: Not applicable.

Informed Consent Statement: Not applicable.

Data Availability Statement: The data presented in this study are available upon request.

Conflicts of Interest: The authors declare no conflicts of interest.

References

- Decong, L.I.; Hong, D.U.; Guomin, W.U.; Xintao, Z.H.; Xionghui, Y.A. Advances in the research of warship structural damage due to inner explosion. Chin. J. Ship Res. 2018, 13, 7–16.
- 2. Chen, Q.; Tao, Y.; Liang, Z.; Yang, J. Analysis of pressure load characteristics of explosive chamber in double cabin model. *Ship Sci. Technol.* **2024**, *46*, 75–79. (In Chinese)
- 3. Li, Y.; Du, Z.P.; Chen, G.C.; Wang, S.P.; Hou, H.L.; Li, X.B.; Zhang, P.; Zhang, L.P.; Kong, X.S.; Li, H.T.; et al. Fundamental problems in blast-induced damage and protection of naval vessels: A state-of-the-art review. *Chin. J. Ship Res.* **2024**, *19*, 3–60. (In Chinese)
- 4. Hu, H.W.; Song, P.; Zhao, S.X.; Feng, H.Y. Progress in Explosion in Confined Space. Chin. J. Energ. Mater. 2013, 21, 539–546.
- 5. Shibue, K.; Sugiyama, Y.; Matsuo, A. Numerical study of the effect on blast-wave mitigation of the quasi-steady drag force from a layer of water droplets sprayed into a confined geometry. *Process Saf. Environ. Prot.* **2022**, *160*, 491–501. [CrossRef]
- 6. Wang, Z.P.; Xu, S.X.; Chen, W.; Le, J.X.; Chai, W.; Li, X.B. Characteristics of shock wave loading inside ship cabin with pressure relief hole. *Chin. J. Ship Res.* **2023**, *18*, 155–162. (In Chinese)
- 7. Trott, B.D.; Backofen, J.; Joseph, E. Design of Explosion Blast Containment Vessels for Explosive Ordnance Disposal Units. In Final Report to Picatinny Arsenal Contract. 1975. Available online: https://apps.dtic.mil/sti/citations/ADB016707 (accessed on 5 August 2024).

8. Weibull, H.R. Pressures recorded in partially closed Cabins at the explosion of TNT charges. *Ann. N. Y. Acad. Sci.* **1968**, 152, 357–361. [CrossRef]

- 9. Esparza, E.D.; Baker, W.E.; Oldham, G.A. Blast Pressures Inside and Outside Suppressive Structures; Department of the Army: Monterey, CA, USA, 1975.
- 10. Anderson, C.E., Jr.; Baker, W.E.; Wauters, D.K.; Morris, B.L. Quasi-static pressure, duration, and impulse for explosions (e.g. HE) in structures. *Int. J. Mech. Sci.* 1983, 25, 455–464. [CrossRef]
- 11. Zhang, Y.; Su, J.; Li, Z.; Jiang, H.; Zhong, K.; Wang, S. Quasi-static pressure characteristic of TNT's internal explosion. *Explos. Shock. Waves* **2018**, *38*, 1429–1434.
- 12. Willauer, H.D.; Ananth, R.; Farley, J.P.; Back, G.G.; Gameiro, V.M.; Kennedy, M.C.; Williams, J.O.C.F.W. *Blast Mitigation Using Water Mist: Test Series II; NRL/MR/6180--09-9182*; Navy Technology Center for Safety and Survivability, Chemistry Division: Calvert County, MD, USA, 2009; p. 12.
- Chen, P.Y.; Hou, H.L.; Liu, G.B.; Zhu, X.; Zhang, G.D. Experimental study on dissipation efficiency of water mist to explosive loading in cabin. J. Milit. Eng. 2018, 39, 927–933. (In Chinese)
- 14. Kong, X.S.; Wang, Z.T.; Kuang, Z.; Zheng, C.; Wu, W. Experimental study on the mitigation effects of confined-blast loading. *Explos. Shock. Waves* **2021**, *41*, 24–37.
- 15. Willauer, H.D.; Ananth, R.; Farley, J.P.; Back, G.G.; Gameiro, V.M.; Kennedy, M.C.; Williams, J.O.C.F.W. Mitigation of TNT and Destex explosion effects using water mist. *J. Hazard. Mater.* **2009**, *165*, 1068–1073. [CrossRef] [PubMed]
- 16. Ananth, R.; Willauer, H.D.; Farley, J.P.; Williams, F.W. Effects of fine water mist on a confined blast. *Fire Technol.* **2012**, *48*, 641–675. [CrossRef]
- 17. Kong, X.; Zhou, H.; Zheng, C.; Liu, H.; Wu, W.; Guan, Z.; Dear, J.P. An experimental study on the mitigation effects of fine water mist on confined-blast loading and dynamic response of steel plates. *Int. J. Impact. Eng.* **2019**, *134*, 103370. [CrossRef]
- 18. Carlson, L.W.; Knight, R.M.; Henrie, J.O. Flame and Detonation Initiation and Propagation in Various Hydrogen-Air Mixtures, with and without Water Spray; Atomics International Div: Los Angeles, CA, USA, 1973.
- 19. Wang, D.W.; Zhang, D.Z.; Li, Y.; Wang, C.L.; Liu, W.X.; Wang, H. Experiment investigation on quasi-static pressure in explosion containment vessels. *Acta Armamentarii* **2012**, *33*, 1493–1497.
- 20. Salter, S.; Parkes, J. Why is Water so Efficient at Suppressing the Effects of Explosions. J. Conv. Weapons Destr. 2018, 22, 56–59.
- 21. Zhang, G.D.; Hou, H.L.; Liu, G.B.; Zhu, X. Research progress of water mist explosion suppression technology in warship compartment. *Ship Sci. Technol.* **2020**, *42*, 1–11.
- 22. Adiga, K.C.; Willauer, H.D.; Ananth, R.; Williams, F.W. Implications of droplet breakup and formation of ultra-fine mist in blast mitigation. *Fire Saf. J.* **2009**, *44*, 363–369. [CrossRef]
- 23. Thomas, G.O.; Jones, A.; Edwards, M.J. Influence of water sprays on explosion development in fuel-air mixtures. *Combust. Sci. Technol.* **1991**, *80*, 47–61. [CrossRef]
- 24. Zhong, W.; Tian, Z.; Zhao, Y. Calculation of the quasi-static temperature of confined explosions in consideration of the effect of the chemical reactions with detonation products. *Explos. Shock Waves* **2015**, *35*, 777–784.

Disclaimer/Publisher's Note: The statements, opinions and data contained in all publications are solely those of the individual author(s) and contributor(s) and not of MDPI and/or the editor(s). MDPI and/or the editor(s) disclaim responsibility for any injury to people or property resulting from any ideas, methods, instructions or products referred to in the content.